Microchimica Acta (2022) 189: 330
https://doi.org/10.1007/s00604-022-05394-3

ORIGINAL PAPER

Magnetic guanidyl–functionalized covalent organic framework composite: a platform for specific capture and isolation of phosphopeptides and exosomes

Bing Wang[1] · Baichun Wang[1] · Quanshou Feng[1] · Xiang Fang[2] · Xinhua Dai[2] · Yinghua Yan[1] · Chuan-Fan Ding[1]

Received: 27 April 2022 / Accepted: 20 June 2022 / Published online: 15 August 2022

Abstract

A guanidine-functionalized (GF) covalent organic framework (COF) nanocomposite has been developed by a post-synthetic approach for specific capture and separation of phosphopeptides and exosomes. The abundant binding sites on COF can immobilize a large number of gold nanoparticles (AuNPs), which can be used to react with amino groups to graft polyethyleneimine (PEI). Finally, Fe_3O_4@COF@Au@PEI-GF is obtained through the reaction of PEI and guanidyl group for phosphopeptides and exosomes detection. This composite shows a low detection limit (0.02 fmol), size exclusion effect (β-casein digests:Albumin from bovine serum protein = 1:10,000), good reusability (10 cycles), and high selectivity (β-casein digests:Albumin from bovine serum digests = 1:10,000). For complex biological sample, 4 phosphopeptides can be successfully identified from human serum. Furthermore, for the first time, we used guanidyl-functionalized probe to capture exosomes in human serum, providing a new method for enriching exosomes. The above experiments showed that Fe_3O_4@COF@Au@PEI-GF not only effectively enrich phosphopeptides and remove macromolecular proteins, but also successfully separate and capture exosomes. This demonstrates the great potential of this composite for the specific enrichment of phosphopeptides and isolation of exosomes.

Keywords Covalent organic framework · Exosomes · Phosphopeptides · Enrichment · Mass spectrometry · SDS-Page · Size exclusion

Introduction

Exosomes, secreted by cells, are membrane vesicles (30–150 nm) that contain complex RNAs, lipids, and proteins [1]. These special membrane vesicles are naturally found in different body fluids [2] and are deemed to be involved in physiological responses such as intercellular communication, signal transduction, and immune regulation [3–5]. As the research on exosomes proceeds, there is evidence that exosomes are participated in the pathology of various diseases [6, 7], and even become important markers of certain diseases [8–10], providing the possibility for early detection of these diseases. To better utilize these unique properties of exosomes for disease diagnosis and treatment [11, 12], it is crucial to isolate and capture exosomes from matrixes, and multiple separation methods have been explored [13]. Ultracentrifugation [14] is a more traditional method; this method can keep exosomes in good activity and shape. At the same time, polymer isolation kits [15] can also be used for the separation of exosomes; this method is simple to operate and does not require special equipment. However, with the continuous innovation of modern separation and analysis technology, the separation and purification of exosomes have put forward higher requirements. Consequently, the methods for the separation of exosomes in samples still need to be further improved, forcing the exploration of innovative methods for low-cost and high-efficiency isolation and capture of exosomes.

✉ Xinhua Dai
daixh@nim.ac.cn

✉ Yinghua Yan
yanyinghua@nbu.edu.cn

[1] Key Laboratory of Advanced Mass Spectrometry and Molecular Analysis of Zhejiang Province, Institute of Mass Spectrometry, School of Material Science and Chemical Engineering, Ningbo University, Ningbo 315211, Zhejiang, China

[2] National Institute of Metrology, Beijing 100084, China

Protein phosphorylation, as a common post-translational modification (PTMs), regulates intercellular communication, neural activity, and immune regulation, and phosphorylated proteins have become specific markers [16–19] for various diseases and even cancers. Phosphorylation not only has an influence on the biogenesis of exosomes [5], but also participates in virtually all biological activities which exosomes are involved in [13], and the physiological and pathological states of primitive cells can be manifested by the changes in proteins in exosomes [14]. Therefore, the research of the phosphorylation associated with exosomes is unusually valuable for elucidating the pathogenesis and pathological process of related diseases [5]. Current methods for enriching phosphopeptides [20] include immunoprecipitation, chemical deposition, and affinity chromatography. Among them, the guanidyl group, as an effective affinity group, has strong non-covalent interactions with phosphate group [21, 22], but there are still relatively few reports on the use of guanidyl groups for the selective separation of phosphopeptides. Besides, to our knowledge, the separation method based on the interaction between guanidyl and phosphate groups present on exosomes phospholipid bilayers has not yet been developed. In this case, the exploration of more novel guanidyl-based functionalized materials would be a good way to enrich phosphopeptides and isolate exosomes.

Covalent organic frameworks (COFs), an emerging promising structure, are porous materials in which tailored building units are connected by covalent bonds [23, 24] to form porous skeletons with periodic structures. COFs have excellent properties [25] such as low density, large specific surface area, and high stability, and have a wide range of applications in catalysis, energy, gas adsorption and separation, and other fields [26–28]. What attracts us is the amazing performance of COFs in the separation and enrichment of phosphopeptides, which stemmed from the controlled pore size, large specific surface area, and regular porosity of COFs [29]. That is, for one thing, more binding sites are endowed in the large specific surface area, and for another, small-sized peptides are trapped in the channel along with the exclusion of large-sized proteins, conferring good selectivity and detection limit. Therefore, the synthesis of more novel COFs materials is still a good attempt.

Herein, a magnetic guanidyl-functionalized (GF) COF composite (Fe_3O_4@COF@Au@PEI-GF) was proposed by layer-by-layer modification on the magnetic core. First, a COF layer was successfully constructed by the aldimine condensation reaction between the aldehyde group on 2,5-divinylterephthalaldehyde and the amino group on 1,3,5-tris(4-aminophenyl) benzene, which endowed a large specific surface area under the condition of ensuring good magnetic properties. Subsequently, gold nanoparticles (AuNPs) were introduced into the surface of magnetic COF by sedimentation method, providing a bridge for the grafting of polyethyleneimine (PEI). So, with the help of Au–N bonds, the modification of PEI not only enhanced the hydrophilic ability of the material, but also provided abundant active sites for the further modification. After functionalizing the guanidyl groups, the synthesized Fe_3O_4@COF@Au@PEI-GF exhibited excellent sensitivity, good stability, and high selectivity for the capture of phosphopeptides and exosomes, showing a wide range of practical application potential.

Experimental section

Chemicals and reagents

2,5-Dihydroxybenzoic acid (DHB), 2,5-divinylterephthalaldehyde (DVA), acetonitrile (ACN), O-methylisourea hemisulfate (OMIU), trisodium citrate dihydrate ($C_6H_5Na_3O_7{\cdot}2H_2O$), anhydrous sodium acetate (NaAc), glycolic acid, 1,3,5-Tris(4-aminophenyl) benzene (TPB), and polyethyleneimine (PEI, M.W. 70000 $g{\cdot}mol^{-1}$, 50 wt% in water) were bought from Aladdin. Albumin from bovine serum (BSA), methanol (MeOH), ethanol (EtOH), β-casein (98%), trypsin, phosphate buffer solution (PBS), acetic acid (HAc), and ethylene glycol were bought from Sigma-Aldrich. Sodium hydroxide (NaOH), iron chloride hexahydrate ($FeCl_3{\cdot}6H_2O$), dithiothreitol (DTT), iodoacetamide (IAA), hydrogen tetrachloroaurate (III) trihydrate ($HAuCl_4{\cdot}3H_2O$), trifluoroacetic acid (TFA), and anhydrous tetrahydrofuran (THF) were purchased from J&K. The serum of the kidney cancer patient was provided by Ningbo medical center Lihuili Hospital.

Synthesis of Fe_3O_4@COF@Au

The specific preparation method of Fe_3O_4@COF can be obtained from the Electronic Support Material. To synthesize AuNPs, $HAuCl_4{\cdot}3H_2O$ (2.5 mL, 20 $mg{\cdot}mL^{-1}$) was dissolved in 122.5 mL of deionized water. When the solution was heated to boiling, trisodium citrate dihydrate (12.5 mL, 38.8 M) was quickly added, and the obtained solution was refluxed for 0.25 h, causing it to turn from light yellow to dark purple.

Fe_3O_4@COF (30 mg) was added to a flask, followed by the addition of 20 mL AuNPs, and the obtained mixture was sonicated for 30 min and mechanically stirred for 1 h. The product (Fe_3O_4@COF@Au) was washed with deionized water and ethanol, and then dried at 60 °C for 24 h under vacuum.

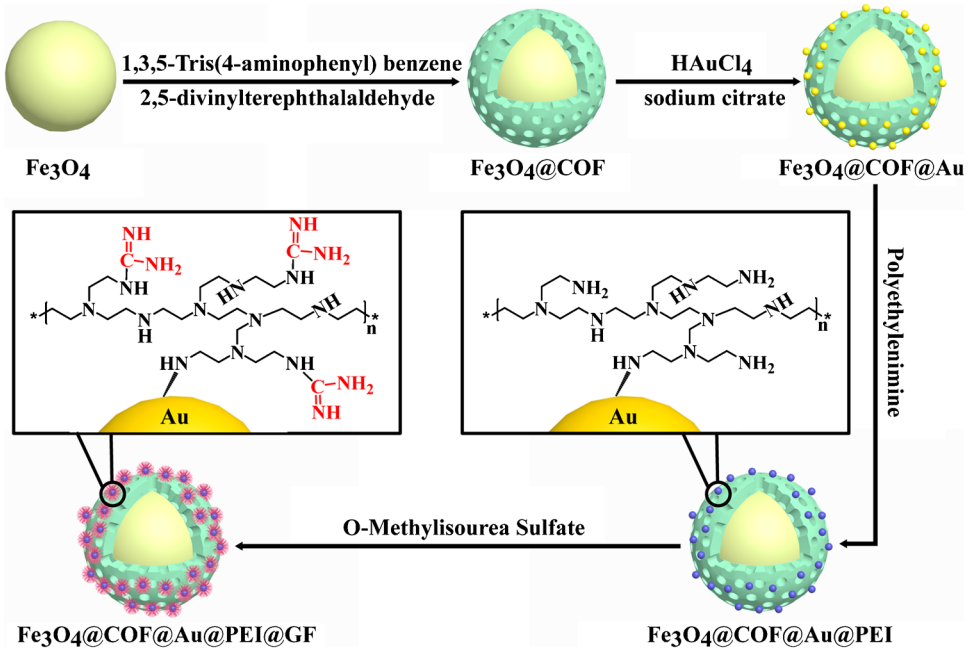

Fig. 1 The schematic representation of the preparation process of Fe_3O_4@COF@Au@PEI-GF composites

Synthesis of Fe_3O_4@COF@Au@PEI

Fe_3O_4@COF@Au (30 mg) was added to 12 mL of deionized water containing PEI (150 mg), and the mixture was shaken at 2500 rpm for 6 h. The obtained Fe_3O_4@COF@Au@PEI was washed four times with deionized water.

Synthesis of Fe_3O_4@COF@Au@PEI-GF

50 mg Fe_3O_4@COF@Au@PEI was dispersed in 50 mL of deionized water containing OMIU (150 mg). The mixture was adjusted to pH = 11 with NaOH, and then mechanically stirred at 60 °C for 24 h. The reaction was terminated by adding 1.65 mL of TFA. The obtained guanidyl-functionalized platform was washed with water and ethanol, and then dried under vacuum at 25 °C.

Specific capture of phosphopeptides from standard protein digests with Fe_3O_4@COF@Au@PEI-GF

First, 500 μg Fe_3O_4@COF@Au@PEI-GF was dispersed in loading buffer consisting of 49% H_2O, 1 M glycolic acid, 1% TFA, and 50% ACN, followed by the addition of 1 μL β-casein digests. After incubation at 37 °C for 45 min, Fe_3O_4@COF@Au@PEI-GF was washed with 100 μL loading buffer to remove the non-phosphopeptides attached to the surface. Next, eluting buffer (10 μL, 10% NH_3•H_2O, w/w) was added, and the mixture was shaken for 30 min at 37 °C to elute the captured phosphopeptides.

Enrichment and isolation of the exosomes from serum

3 mg of Fe_3O_4@COF@Au@PEI-GF was added in 10 μL of human serum. Next, the mixture was shaken at 4 °C for 45 min to capture the exosomes in serum, and then washed with PBS solution to remove impurities. Finally, eluting buffer (20 μL, 0.4 M NH_3•H_2O) was added, and the eluent was obtained by incubation at 4 °C for 30 min.

Results and discussion

The synthesis and characterization of Fe_3O_4@COF@Au@PEI-GF

The preparation process of Fe_3O_4@COF@Au@PEI-GF is shown in Fig. 1. First, Fe_3O_4 nanoparticles are prepared by the solvothermal method. At room temperature, via the condensation of amino and aldehyde groups, 1,3,5-tris(4-aminophenyl) benzene and 2,5-divinylterephthalaldehyde are employed as ligands to form a porous COF layer on the magnetic core Fe_3O_4. Then, the sedimentation method enables AuNPs to be grafted on the surface of the magnetic COF, which acts as a bridge to allow PEI access. Subsequently, PEI is immobilized on the surface of the AuNPs by forming Au–N bonds. Finally, guanidyl-functionalized material Fe_3O_4@COF@Au@PEI-GF is prepared through the nucleophilic substitution of methoxy groups for amino groups on PEI.

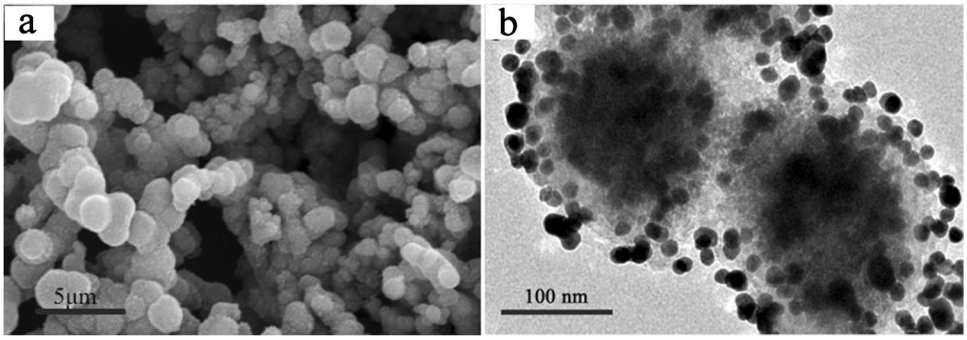

Fig. 2 **a** SEM image of Fe_3O_4@COF@Au@PEI-GF; **b** TEM image of Fe_3O_4@COF@Au@PEI-GF

A series of characterizations were performed on Fe_3O_4@COF@Au@PEI-GF to verify the successful synthesis. First, the microstructures of this material were visualized through SEM and TEM. As shown in Fig. 2a, the final product are rough-surfaced spheres with a diameter of approximately 200 nm. In Fig. 2b, it is shown that the Fe_3O_4 are encapsulated by COF to form a uniform core–shell structure, and a lot of AuNPs with an approximate diameter of about 15 nm are also embedded on the surface of the material. Additionally, the crystal structure of Fe_3O_4@COF@Au@PEI-GF was characterized using X-ray diffraction (XRD). As can be seen from Fig. S1, the characteristic peaks [30] of Fe_3O_4 are at 30.1° (220), 35.5° (311), 43.53° (400), 53.91° (422), 57.1° (511), and 62.0° (440), and the characteristic peaks [31, 32] of AuNPs are at 38.1° (111), 44.4° (200), and 64.7° (221). The results of XRD show that the prepared material has good crystallinity. The presence of C, N, O, Fe, and Au elements is observed (Fig. S2) in the energy dispersive X-ray spectra (EDX), which indicates that Fe_3O_4@COF@Au@PEI-GF was successfully synthesized. Fourier-transform infrared spectroscopy (FT-IR) was further verified the success of the entire material process. As shown in Fig. S3, the FT-IR spectra of all products shows an absorption band (green absorption band) at 1618 cm^{-1}, which is due to the C = N stretching vibration in COF [33], demonstrating the COF is successfully synthesized on the surface of Fe_3O_4. The FT-IR spectra of Fe_3O_4@COF@Au@PEI shows new absorption bands [34] (purple absorption band) at 2935 cm^{-1} and 1455 cm^{-1}, proving that the successful modification of PEI on the surface of AuNPs. A new peak (yellow absorption band) at 1114 cm^{-1} is attributed to the C-N bond stretching vibrations [35] from guanidyl groups. The above series of characterization fully demonstrates the successful development of Fe_3O_4@COF@Au@PEI-GF.

Research on the ability of Fe_3O_4@COF@Au@PEI-GF for selective enrichment of phosphopeptides

In order to test the selectivity of the material, trypsin digested of *β*-casein was used as the analyte. Firstly, directly analyze the trypsin digested of *β*-casein with MALDI-TOF MS (Fig. S4a), and most of the peaks obtained are non-phosphopeptides, with only one phosphopeptide peak of low intensity detected. However, after treated with Fe_3O_4@COF@Au@PEI-GF, eleven peaks belonging to phosphopeptides are identified in the elute due to the non-covalent interaction between the guanidyl groups and the phosphate groups (Fig. S4b), and the relevant information is listed in Table S1. The experiment shows that the synthesized guanidyl-based affinity material has a good enrichment ability and affinity for phosphopeptides.

To detect the detection limit of Fe_3O_4@COF@Au@PEI-GF towards phosphopeptides, different contents (20, 2, 0.2, and 0.02 fmol) of *β*-casein digests were treated with the material. When the *β*-casein digests concentration is diluted to 20 fmol, after enriched by the obtained Fe_3O_4@COF@Au@PEI-GF, all signals of the above phosphopeptides can be identified (Fig. 3a). After the concentration is further diluted to 2 fmol (Fig. 3b), ten peaks of phosphopeptides still appears, indicating that Fe_3O_4@COF@Au@PEI-GF can maintain its good capture capability at a low content of β-casein digests. Even if the contents are reduced to 0.2 fmol (Fig. 3c) and 0.02 fmol (Fig. 3d), 4 and 1 peaks of phosphopeptides can still be observed, respectively. The above experiments demonstrate that the nanosphere Fe_3O_4@COF@Au@PEI-GF has higher sensitivity for phosphopeptides.

Furthermore, the reusability of Fe_3O_4@COF@Au@PEI-GF was verified, and the results are shown in Fig. S5. To make the experiment more accurate, after each enrichment, the nanocomposite was washed several times with the loading buffer and ammonia aqueous solution, respectively, to remove the residues. According to the comparison of multiple cycles, the results of the fourth and seventh cycles (Fig. S5b and S5c) are almost the same as the first cycle (Fig. S5a). Even in the result of tenth cycle (Fig. S5d), the numbers and intensities of the phosphopeptide peaks in the spectrum also barely changed, showing that Fe_3O_4@COF@Au@PEI-GF has a good reusability.

The selectivity of Fe_3O_4@COF@Au@PEI-GF for phosphopeptides was investigated by enriching phosphopeptides in different molar ratios of *β*-casein digests and BSA. When Fe_3O_4@COF@Au@PEI-GF is applied to enrich *β*-casein:

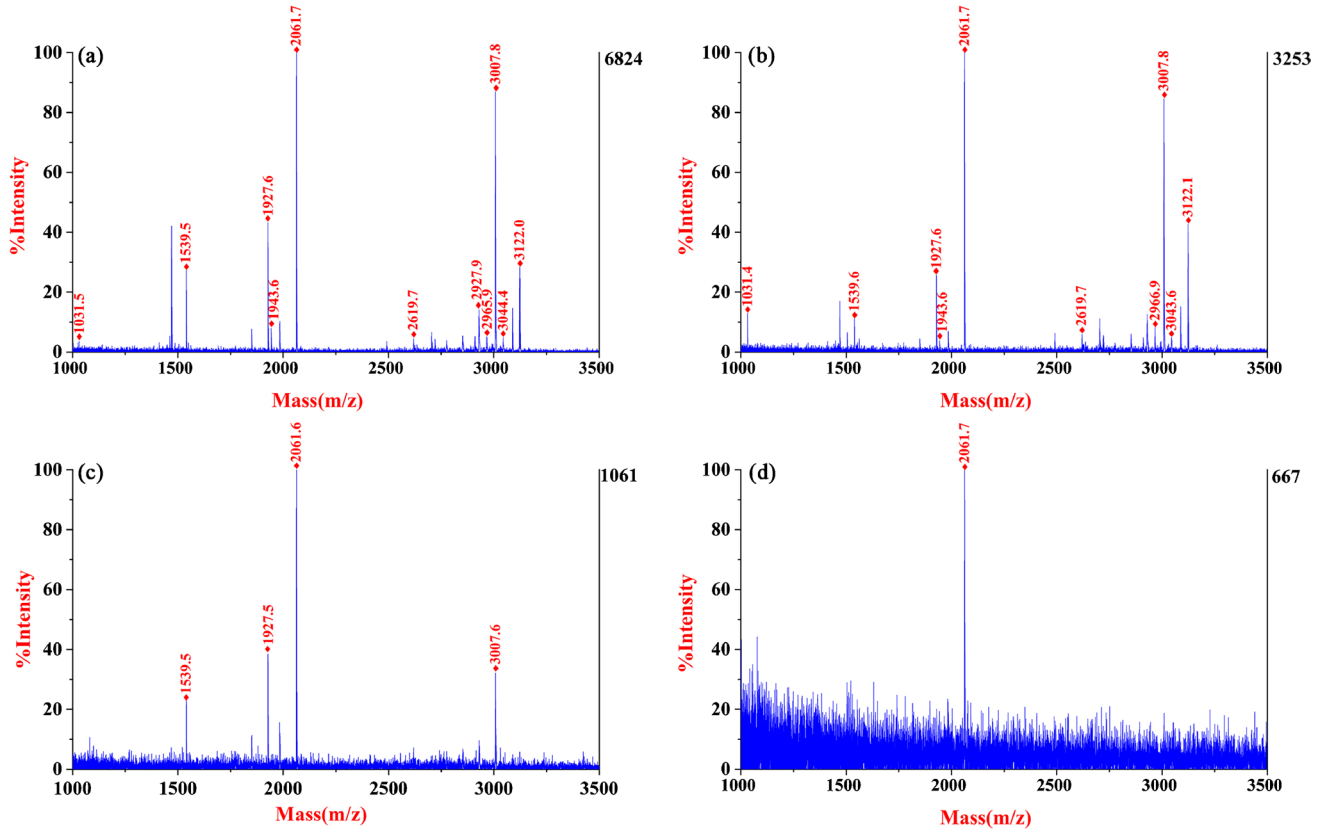

Fig. 3 MALDI-TOF MS spectra of β-casein digests with different contents after the enrichment by Fe_3O_4@COF@Au@PEI-GF: **a** 20 fmol, **b** 2 fmol, **c** 0.2 fmol, and **d** 0.02 fmol. Diamond indicates the peak of phosphopeptide

BSA digests with a molar ratio of 1:1000 (Fig. 4a); four phosphopeptide peaks can be detected by MALDI-TOF MS. Notably, even if the molar ratio is increased to 1:2000 and 1:5000, three and two phosphopeptide peaks can still be detected (Fig. 4b and c), respectively. After the molar ratio is increased to 1:10,000, although the intensities and number of the phosphopeptide peaks decreased, a signal is still detected against a clear background (Fig. 4d). These results indicate that Fe_3O_4@COF@Au@PEI-GF has an outstanding selectivity for phosphopeptides.

The size exclusion effect was studied based on the mesoporous structure [36] in the COF shell of Fe_3O_4@COF@Au@PEI-GF. The mixtures of bovine serum albumin (BSA) protein and *β*-casein digests with different molar ratios were used for validation, and the results are shown in Fig. S6. When the molar ratio of the BSA protein and β-casein digests is 1000:1 (Fig. S6a), seven phosphopeptide peaks can be observed. After the molar ratio is increased to 2000:1 (Fig. S6b), the peaks of phosphopeptides still dominate the spectrum, and five signals with a signal-to-noise ratio above 3 can be seen. In the results of the molar ratios of 5000:1 and 10,000:1 (Fig. S6c and S6d), although the signals of non-phosphopeptides are greatly improved, three and one signals of phosphopeptides are still observed, respectively. This is attributed to the pore size selectivity of COF from Fe_3O_4@COF@Au@PEI-GF, and phosphopeptides of small size could still be captured efficiently.

The loading capacity of Fe_3O_4@COF@Au@PEI-GF for phosphopeptides was judged by observing the intensity changes of three representative phosphopeptide peaks. The determination was performed by changing the amount of material by fixing the amount of *β*-casein. The results are shown in Fig. S7, the loading capacity of the material for phosphopeptides increased continuously from 10 to 25 μg, and reached saturation when the amount of material was 25 μg. In order to further verify whether the material reached a saturated state, the supernatant after incubation was taken for enrichment analysis again. When the amount of material was 20 μg, the phosphopeptide peak could still be detected (Fig. S8a). However, when the amount of material reached 25 μg, no phosphopeptide peak was detected (Fig. S8b). This result demonstrates that the material reaches saturation at 25 μg. According to the above results, it can be calculated that the loading capacity of Fe_3O_4@COF@Au@PEI-GF is 30 $mg \cdot g^{-1}$.

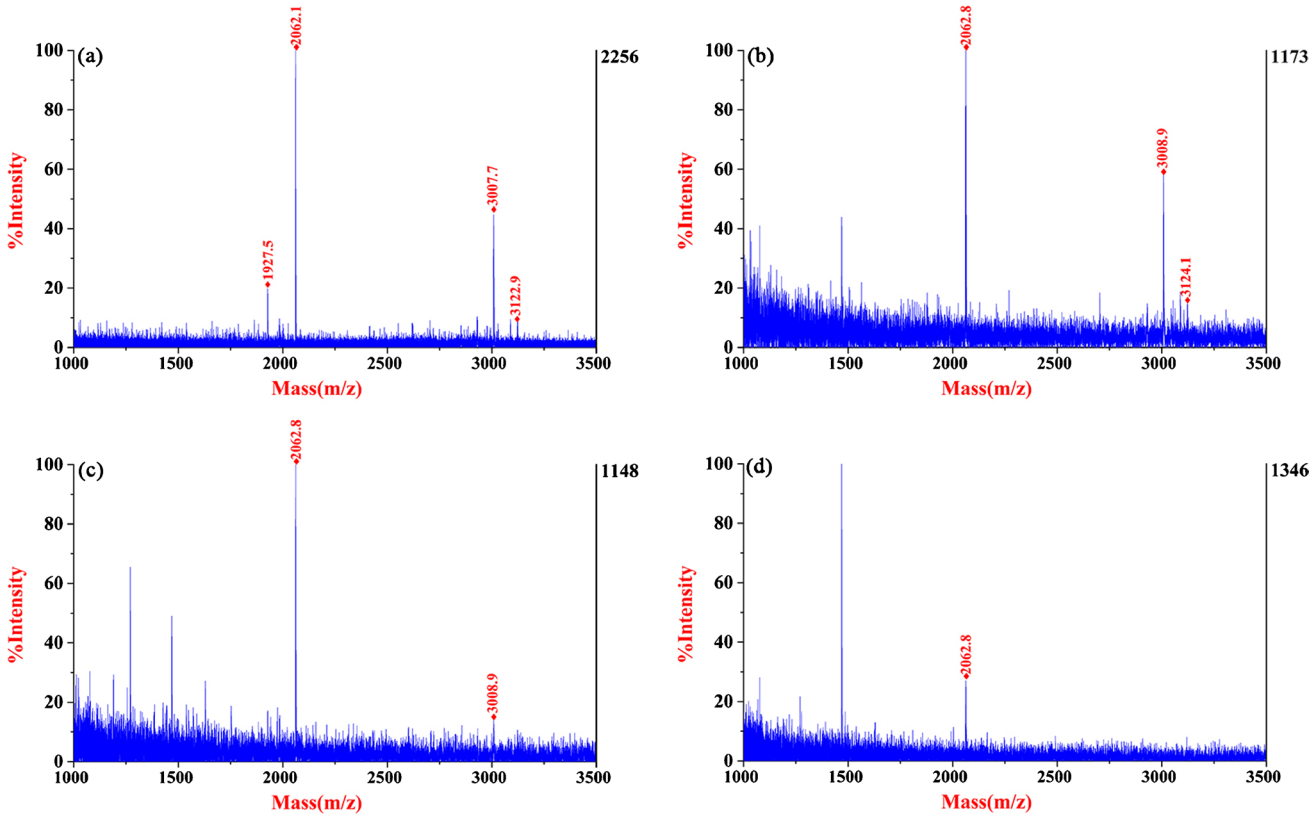

Fig. 4 MALDI-TOF MS spectra of the mixture of β-casein digests and BSA digests with different molar ratios after the enrichment with Fe_3O_4@COF@Au@PEI-GF: **a** 1:1000 (β-casein (2 pmol):BSA (2000 pmol)), **b** 1:2000 (β-casein (2 pmol):BSA (4000 pmol)), **c** 1:5000 (β-casein (2 pmol):BSA (10,000 pmol)), and **d** 1:10,000 (β-casein (2 pmol):BSA (20,000 pmol)). Diamond indicates the peak of phosphopeptide

Table S2 displays the detailed comparative information of guanidyl-functionalized (GF) COF materials for the enrichment of phosphopeptides. By comparison, it can be seen that the Fe_3O_4@COF@Au@PEI-GF has several excellent performances, such as reusability, selectivity, and limit of detection. According to the comparison with the materials in the table, it can be seen that Fe_3O_4@COF@Au@PEI-GF material has better selectivity and lower detection limit. Furthermore, the modification of the PEI group improves the hydrophilicity of the material and provides abundant active sites for further modification. Therefore, the successful preparation of Fe_3O_4@COF@Au@PEI-GF indicates that the material has good applicability in phosphoproteomic studies. Although the material is surprising for its application to phosphopeptides, there are still some limitations. For example, organic reagents are used many times during the synthesis, which contradicts the idea of green chemistry. It will be a nice step forward if the materials could be prepared under environmentally friendly conditions.

Research on the ability of Fe_3O_4@COF@Au@PEI-GF to enrich phosphopeptide from biological samples (human serum)

Healthy human serum and renal cancer patient serum were chosen as actual samples to verify whether Fe_3O_4@COF@Au@PEI-GF could be used to analyze complex samples. When human serum is analyzed directly before enrichment (Fig. 5a and c), the peaks of phosphopeptides are not found in the spectrum, and spectra are dominated by non-phosphopeptides. After enrichment with Fe_3O_4@COF@Au@PEI-GF, four characteristic phosphopeptide peaks are captured in human serum (Fig. 5b and d), but it could be clearly seen that the phosphopeptides from human serum were expressed differently between healthy and kidney cancer individuals, especially the phosphopeptide peaks at m/z = 1389.5 and 1616.6. Details information is shown in Table S3. These results indicate the great potential for practical applications of the Fe_3O_4@COF@Au@PEI-GF composite.

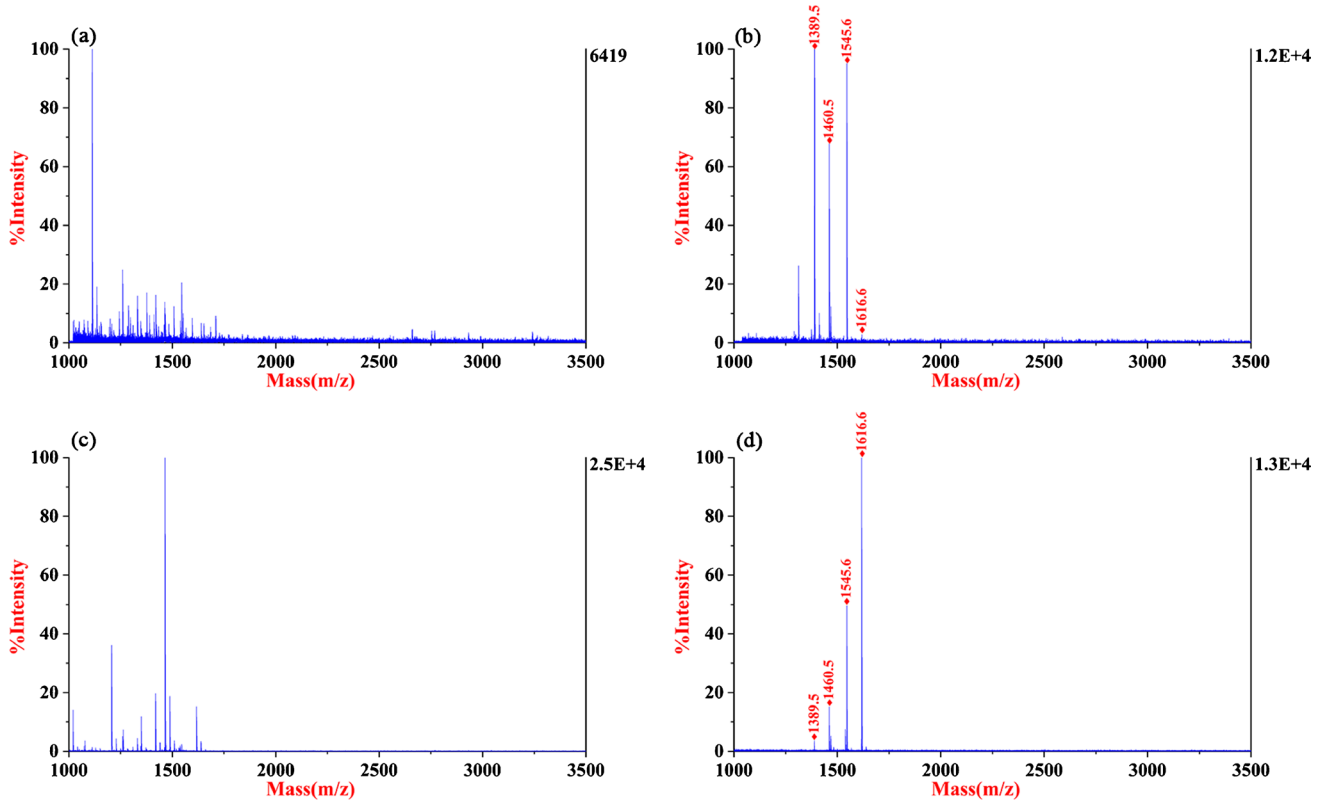

Fig. 5 MALDI-TOF mass spectra of phosphopeptides from human serum: **a** healthy human serum before enrichment, **b** after enrichment by Fe_3O_4@COF@Au@PEI-GF, **c** patient serum before enrichment, and **d** after enrichment by Fe_3O_4@COF@Au@PEI-GF. Diamond indicates the peak of phosphopeptide

Application of Fe_3O_4@COF@Au@PEI-GF for exosome isolation from serum

Fe_3O_4@COF@Au@PEI-GF was enriched exosomes in serum samples at 4 °C. To verify the feasibility of the method for isolating exosomes from serum, some methods were selected for evaluation. First, the morphological states of the exosomes captured by Fe_3O_4@COF@Au@PEI-GF were observed by TEM images. The TEM image (Fig. S9a) showed that the exosomes were vesicle-like, and the diameter of the exosomes was approximately 30–150 nm, which was consistent with literature reports. Second, the nanoparticle tracking analysis (NTA) system was used to detect the concentration of exosomes isolated from human serum. NTA is one of the means to characterize exosomes, which is a technique for real-time dynamic tracking of the Brownian motion of nanoparticles. As shown in Fig. S9b, the exosome concentration was 1.19×10^9 particles·mL^{-1}. In addition, sodium dodecyl sulfate polyacrylamide gelelectrophoresis (SDS-PAGE) further verified the feasibility of Fe_3O_4@COF@Au@PEI-GF method to isolate exosomes in serum. As seen in Fig. 6 ①, a band of uromodulin (UMOD) can be observed before capture, while only weak or even no bands were observed for the exosome marker protein. That is, despite the presence of exosomes in serum, exosome marker proteins could not be directly detected by SDS-PAGE due to

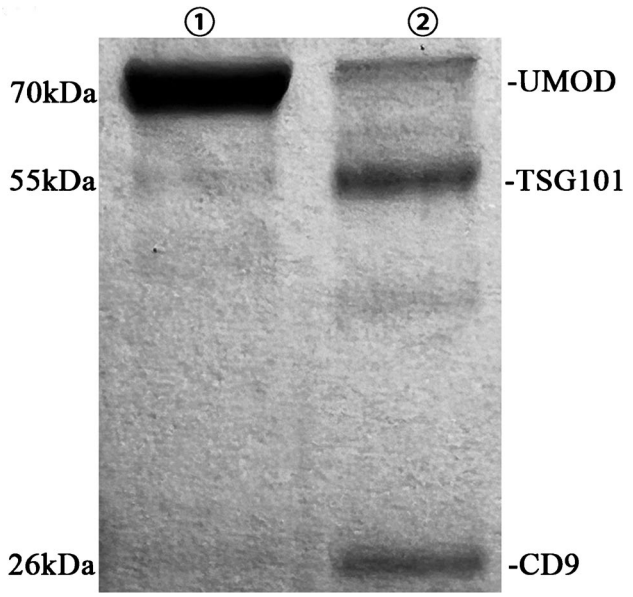

Fig. 6 SDS-PAGE results of marker proteins in exosomes of serum: (①) before, and (②) after captured by Fe_3O_4@COF@Au@PEI-GF

the low concentration of exosomes, and it has been reported [37] that UMOD, a high molecular weight protein, will hinder the separation of exosomes. After the capture and separation of exosomes in serum by the composite Fe_3O_4@COF@Au@PEI-GF and the detection of the eluent by sodium dodecyl sulfate polyacrylamide gel electrophoresis (Fig. 6 ②), it appears the clear strips of exosome marker proteins (TSG101 and CD9) [38], while the band of UMOD becomes shallower. This specific capture can be explained by the interaction between guanidyl groups and the phospholipid bilayer of exosomes. The above experimental results showed that Fe_3O_4@COF@Au@PEI-GF could enrich and separate the exosomes in serum, providing a practical avenue for the development of its novel and convenient separation strategy.

Conclusions

In conclusion, based on the post-synthetic functionalization route, Fe_3O_4@COF@Au@PEI-GF is obtained by step-by-step modification on the substrate material Fe_3O_4. Because of the large surface area, regular pore structure, high stability, and superior magnetic properties of the Fe_3O_4@COF@Au@PEI-GF, this material exhibits excellent performance on enriching phosphopeptides, such as excellent sensitivity (0.02 fmol) and good reusability (10 cycles). Furthermore, with the help of porous COF layers and functionalized guanidine groups, the platform not only has stunning selectivity (1:10,000) and size exclusion effect (1:10,000), but also captures phosphopeptides from complex systems (human serum). This guanidine-functionalized platform will show a broad prospect in the application of phosphoproteome. The limitation of material is that it does not conform to the concept of green chemistry. If possible, it is best to prepare the synthesis in an environmentally friendly system. In addition, this guanidyl-functionalized probe is also able to successfully capture and isolate exosomes in serum, providing a richer and effective enrichment strategy and wide application potential.

Supplementary Information The online version contains supplementary material available at https://doi.org/10.1007/s00604-022-05394-3.

Funding This work is supported by National Natural Science Foundation of China (21927805), Natural Science Foundation of Zhejiang Province (LY22B050008), Major Science and Technology Projects in Ningbo (2020Z090), and the K. C. Wong Magna Fund in Ningbo University.

Declarations

Conflict of interest The authors declare no competing interests.

References

1. Melo SA, Luecke LB, Kahlert C, Fernandez AF, Gammon ST, Kaye J, LeBleu VS, Mittendorf EA, Weitz J, Rahbari N, Reissfelder C, Pilarsky C, Fraga MF, Worms DP, Kalluri R (2015) Glypican-1 identifies cancer exosomes and detects early pancreatic cancer. Nature 523:177-U82. https://doi.org/10.1038/nature14581
2. Tauro BJ, Greening DW, Mathias RA, Ji H, Mathivanan S, Scott AM, Simpson RJ (2012) Comparison of ultracentrifugation, density gradient separation, and immunoaffinity capture methods for isolating human colon cancer cell line LIM1863-derived exosomes. Methods 56:293–304. https://doi.org/10.1016/j.ymeth.2012.01.002
3. Wei HX, Chen JY, Wang SL, Fu FH, Zhu X, Wu CY, Liu ZJ, Zhong GX, Lin JH (2019) A nanodrug consisting of doxorubicin and exosome derived from mesenchymal stem cells for osteosarcoma treatment in vitro. Int J Nanomedicine 14:8603–8610. https://doi.org/10.2147/IJN.S218988
4. Webber J, Steadman R, Mason MD, Tabi Z, Clayton A (2010) Cancer exosomes trigger fibroblast to myofibroblast differentiation. Cancer Res 70:9621–9630. https://doi.org/10.1158/0008-5472.CAN-10-1722
5. Xiong FF, Jia JX, Ma JT, Jia Q (2022) Glutathione-functionalized magnetic thioether-COFs for the simultaneous capture of urinary exosomes and enrichment of exosomal glycosylated and phosphorylated peptides. Nanoscale 14:853–864. https://doi.org/10.1039/d1nr06587d
6. Kang YT, Kim YJ, Bu J, Cho YH, Han SW, Moon BI (2017) High-purity capture and release of circulating exosomes using an exosome-specific dual-patterned immunofiltration (ExoDIF) device. Nanoscale 9:13495–13505. https://doi.org/10.1039/c7nr04557c
7. Hwang DW (2019) Perspective in nuclear theranostics using exosome for the brain. Med Mol Imaging 53:108–114. https://doi.org/10.1007/s13139-018-00567-6
8. Lin SJ, Yu ZX, Chen D, Wang ZG, Miao JM, Li QC, Zhang DY, Song J, Cui DX (2020) Progress in microfluidics-based exosome separation and detection technologies for diagnostic applications. Small 16:1903916. https://doi.org/10.1002/smll.201903916
9. Singh K, Nalabotala R, Koo KM, Bose S, Nayak R, Shiddiky MJA (2021) Separation of distinct exosome subpopulations: isolation and characterization approaches and their associated challenges. Analyst 146:3731–3749. https://doi.org/10.1039/d1an00024a
10. Sun NR, Yu HL, Wu H, Shen XZ, Deng CH (2021) Advanced nanomaterials as sample technique for bio-analysis. Trac-Trends Anal Chem 135:116168. https://doi.org/10.1016/j.trac.2020.116168
11. Khodashenas S, Khalili S, Moghadam MF (2019) A cell ELISA based method for exosome detection in diagnostic and therapeutic applications. Biotechnol Lett 41:523–531. https://doi.org/10.1007/s10529-019-02667-5
12. Riva P, Battaglia C, Venturin M (2019) Emerging role of genetic alterations affecting exosome biology in neurodegenerative diseases. Int J Mol Sci 20:4113. https://doi.org/10.3390/ijms20174113
13. Zhang N, Hu XF, Chen HL, Deng CH, Sun NAR (2021) Specific enrichment and glycosylation discrepancy profiling of cellular exosomes by dual-affinity probe. Chem Commun 57:6249–6252. https://doi.org/10.1039/d1cc01530c
14. Zhang N, Sun NR, Deng CH (2020) A hydrophilic magnetic MOF for the consecutive enrichment of exosomes and exosomal phosphopeptides. Chem Commun 56:13999–14002. https://doi.org/10.1039/d0cc06147f

15. Cao F, Gao Y, Chu Q, Wu Q, Zhao L, Lan T, Zhao L (2019) Proteomics comparison of exosomes from serum and plasma between ultracentrifugation and polymer-based precipitation kit methods. Electrophoresis 40:3092–3098. https://doi.org/10.1002/elps.201900295
16. Sun NR, Wang JW, Yao Z, Chen HM, Deng CH (2019) Magnetite nanoparticles coated with mercaptosuccinic acid-modified mesoporous titania as a hydrophilic sorbent for glycopeptides and phosphopeptides prior to their quantitation by LC-MS/MS. Microchim Acta 186:159. https://doi.org/10.1007/s00604-019-3274-3
17. Sun NR, Wang ZD, Wang JW, Chen HM, Wu H, Shen S, Deng CH (2019) Hydrophilic tripeptide combined with magnetic titania as a multipurpose platform for universal enrichment of phospho- and glycopeptides. J Chromatogr A 1595:1–10. https://doi.org/10.1016/j.chroma.2019.02.039
18. Liu B, Wang BC, Yan YH, Tang KQ, Ding CF (2021) Efficient separation of phosphopeptides employing a Ti/Nb-functionalized core-shell structure solid-phase extraction nanosphere. Microchim Acta 188:32. https://doi.org/10.1007/s00604-020-04652-6
19. Chu HM, Zheng HY, Yao JZ, Sun NR, Yan GQ, Deng CH (2020) Magnetic metal phenolic networks: expanding the application of a promising nanoprobe to phosphoproteomics research. Chem Commun 56:11299–11302. https://doi.org/10.1039/d0cc04615a
20. Du JL, Yan YH, Tang KQ, Ding CF (2021) Modified carbon nanotubes decorated with ZIFs as new immobilized metal ion affinity chromatography platform for enrichment of phosphopeptides. ChemistrySelect 6:1313–1319. https://doi.org/10.1002/slct.202004650
21. Luo B, Zhou XX, Jiang PP, Yi QY, Lan F, Wu Y (2018) PAMA-Arg brushes-functionalized magnetic composite nanospheres for highly effective enrichment of the phosphorylated biomolecules. J Mater Chem B 6:3969–3978. https://doi.org/10.1039/c8tb00705e
22. Jiang DD, Duan LM, Jia Q, Liu JH (2020) Glycocyamine functionalized magnetic layered double hydroxides with multiple affinity sites for trace phosphopeptides enrichment. Anal Chim Acta 1136:25–33. https://doi.org/10.1016/j.aca.2020.07.057
23. Xie ZH, Yan YH, Tang KQ, Ding CF (2022) Post-synthesis modification of covalent organic frameworks for ultrahigh enrichment of low-abundance glycopeptides from human saliva and serum. Talanta 236:122831. https://doi.org/10.1016/j.talanta.2021.122831
24. Gao CH, Bai J, He YT, Zheng Q, Ma WD, Lei ZX, Zhang MY, Wu J, Fu FF, Lin Z (2019) Postsynthetic functionalization of Zr^{4+}-immobilized core−shell structured magnetic covalent organic frameworks for selective enrichment of phosphopeptides. ACS Appl Mater Interfaces 11:13735–13741. https://doi.org/10.1021/acsami.9b03330
25. Chen L, He YT, Lei ZX, Gao CL, Xie Q, Tong P, Lin Z (2018) Preparation of core-shell structured magnetic covalent organic framework nanocomposites for magnetic solid-phase extraction of bisphenols from human serum sample. Talanta 181:296–304. https://doi.org/10.1016/j.talanta.2018.01.036
26. You LJ, Xu K, Ding GJ, Shi XM, Li JM, Wang SY, Wang JB (2020) Facile synthesis of Fe_3O_4@COF covalent organic frameworks for the adsorption of bisphenols from aqueous solution. J Mol Liq 320:114456. https://doi.org/10.1016/j.molliq.2020.114456
27. Baldwin LA, Crowe JW, Pyles DA, McGrier PL (2016) Metalation of a mesoporous three-dimensional covalent organic framework. J Am Chem Soc 138:15134–15137. https://doi.org/10.1021/jacs.6b10316
28. Lu YY, Wang XL, Wang LL, Zhang W, Wei JJ, Lin JM, Zhao RS (2021) Room-temperature synthesis of amino-functionalized magnetic covalent organic frameworks for efficient extraction of perfluoroalkyl acids in environmental water samples. J Hazard Mater 407:124782. https://doi.org/10.1016/j.jhazmat.2020.124782
29. Wang JX, Li J, Gao MX, Zhang XM (2018) Recent advances in covalent organic frameworks for separation and analysis of complex samples. TrAC Trends Anal Chem 108:98–109. https://doi.org/10.1016/j.trac.2018.07.013
30. Fu QB, Jiang HL, Qiao LQ, Sun X, Wang ML, Zhao RS (2020) Effective enrichment and detection of trace polybrominated diphenyl ethers in water samples based on magnetic covalent organic framework nanospheres coupled with chromatography-mass spectrometry. J Chromatogr A 1630:461534. https://doi.org/10.1016/j.chroma.2020.461534
31. Ren JF, Shen S, Pang ZQ, Lu XH, Deng CH, Jiang XG (2011) Facile synthesis of superparamagnetic Fe_3O_4@Au nanoparticles for photothermal destruction of cancer cells. Chem Commun 47:11692–11694. https://doi.org/10.1039/c1cc15528h
32. Ma YY, Zhao YX, Xu XT, Ding SJ, Li YH (2021) Magnetic covalent organic framework immobilized gold nanoparticles with high-efficiency catalytic performance for chemiluminescent detection of pesticide triazophos. Talanta 235:122798. https://doi.org/10.1016/j.talanta.2021.122798
33. Yang CJ, Yu HL, Hu XF, Chen HL, Wu H, Deng CH, Sun NR (2021) Gold-Doped covalent-organic framework reveals specific serum metabolic fingerprints as point of Crohn's disease diagnosis. Adv Funct Mater 31:2105478. https://doi.org/10.1002/adfm.202105478
34. Jiang B, Qu YY, Zhang LH, Liang Z, Zhang YK (2016) 4-Mercaptophenylboronic acid functionalized graphene oxide composites: preparation, characterization and selective enrichment of glycopeptides. Anal Chim Acta 912:41–48. https://doi.org/10.1016/j.aca.2016.01.018
35. Liu HL, Lian B (2018) A guanidyl-functionalized TiO_2 nanoparticle-anchored graphene nanohybrid for enhanced capture of phosphopeptides. RSC Adv 8:29476–29481. https://doi.org/10.1039/c8ra90074d
36. Li JY, Zhang S, Gao W, Hua Y, Lian HZ (2020) Guanidyl-Functionalized magnetic bimetallic MOF nanocomposites developed for selective enrichment of phosphopeptides. ACS Sustainable Chem Eng 8:16422–16429. https://doi.org/10.1021/acssuschemeng.0c04118
37. Zhang N, Sun NR, Deng CH (2021) Rapid isolation and proteome analysis of urinary exosome based on double interactions of Fe_3O_4@TiO_2-DNA aptamer. Talanta 221:121571. https://doi.org/10.1016/j.talanta.2020.121571
38. Smolarz M, Pietrowska M, Matysiak N, Mielańczyk Ł, Widłak P (2019) Proteome profiling of exosomes purified from a small amount of human serum: the problem of co-purified serum components. Proteomes 7(2):18. https://doi.org/10.3390/proteomes7020018